8/11

Cosmic Ray Project

APPLIED PHYSICS LABORATORY

A DIVISION OF THE DEPARTMENT OF PHYSICS
UNIVERSITY OF WASHINGTON

Cosmic Ray Protons at 3.4 Kilometers and the Nuclear Absorption of Protons in Lead

TECHNICAL REPORT

OFFICE OF NAVAL RESEARCH
CONTRACT N8 onr52008

APPLIED PHYSICS LABORATORY

UNIVERSITY OF WASHINGTON

A Division of the Department of Physics

COSMIC RAY PROTONS AT 3.4 KILOMETERS AND THE NUCLEAR ABSORPTION OF PROTONS IN LEAD

By Gerald R. Garrison*, C. E. Miller, J. E. Henderson, F. M. Charbonnier, D. S. Potter and W. M. Sandstrom

TECHNICAL REPORT

OFFICE OF NAVY RESEARCH

CONTRACT N8onr 52008

Acknowledgment is made to the Bureau of Ordnance, Navy Department for support of the early stages of this research under Contract NOrd 7818.

Approved

Jos. E. Henderson

J. E. Henderson, Director
Applied Physics Laboratory

*The physical material of this report was presented by G. R. Garrison as a dissertation in partial fulfillment of the requirements for the Degree of Doctor of Philosophy of the Graduate School of the University of Washington.

ACKNOWLEDGEMENT

The high altitude work described here was carried out on the grounds of the Climax Molybdenum Company at Fremont Pass in Colorado. The generous cooperation of C. S. Abrams, General Manager, and other personnel of this company is gratefully acknowledged. Important contributions to the research have also been made by Don Eng, electronic technician, and Elmer Wright, instrument maker, for our staff.

TABLE OF CONTENTS

TABLE OF CONTENTS (continued)

LIST OF TABLES

LIST OF FIGURES

COSMIC RAY PROTONS AT 3.4 KILOMETERS AND THE NUCLEAR ABSORPTION OF PROTONS IN LEAD

PART I

INTRODUCTION

Until recent years the cosmic ray hard component at lower altitudes was considered to consist almost entirely of mu mesons. Experiments had failed to detect the substantial number of protons present in the hard component because of the difficulty of distinguishing between high energy protons and mesons. At the same time the soft component, defined by its rapid absorption of matter, was considered to consist almost entirely of cascade radiation (electrons, positrons and photons). Here the complexity of shower phenomena made compositional studies difficult so that the substantial number of protons present in the soft component had not been detected. As the primary radiation is considered to consist mainly of protons it was clear that at some altitude these should begin to be present in appreciable numbers.

Detection of protons by methods based on the density of cloud chamber tracks had shown a very small percentage of this radiation to be present even at 4000 meters altitude (References 5 and 6). Subsequent work performed by Miller, Potter and Todd (1,3) has indicated the difficulty of obtaining reliable information by this means. In 1948, cloud chamber observations at 30,000 feet made by Adams, Anderson et al (7) indicated the presence of large numbers of protons of about 0.5 Bev/c momentum. The nature and statistics of the experiment were not adequate to give detailed information, nor were absolute intensities obtained.

Since that time a major portion of the effort of this laboratory has been directed towards obtaining detailed information on the intensity and energy distribution of protons at sea level and mountain altitudes. In the first observation made in 1948 (3) a momentum spectrum of the total non-cascade radiation to a momentum of 2.5 Bev/c was obtained. Substantial numbers of protons were recognized by their track density, but the method was considered too subjective and the apparent track density too variable to give reliable information. Subsequent observations made in 1949 (4) were directed towards obtaining complete meson and proton separation in limited range intervals.

The basic objective of the present work is to measure the proton momentum spectrum at high momenta. This work,

when coupled with that of Todd, gives a reliable momentum spectrum over the entire interval from 0.7 to 2.0 Bev/c. In addition, information is obtained on the nuclear interaction path length of protons in lead.

PART II

EXPERIMENTAL METHOD

A. Possible Techniques of Proton Detection

In principle, any technique capable of measuring the amount of ionization produced when charged particles traverse matter can be adapted to distinguish protons from mesons. While many such techniques exist, most of them suffer from too small sensitivity or too large statistical fluctuations to be capable of distinguishing a single particle traversal of minimum ionization from one of several times minimum. Also, as most techniques indicate only total ionization, distinction is not made between large pulses due to heavily ionizing single particles and those due to simultaneous traversal by several particles. The following is a summary of available methods, other than the one used here which will be treated in Section B.

1. Ionization chambers. These measure total ionization produced but are too insensitive to show the pulse size for a single particle. They can, however, detect large stars produced by protons in the chamber walls and so measure the intensity of the star-producing radiation if provision is made for good protection against electron showers.

2. Scintillation counters. These are capable of showing the pulse size for a single particle traversal but suffer from too large a statistical fluctuation in pulse size to distinguish protons from mesons. This statistical fluctuation results from added ionization produced by large energy knock-on electrons. They can, however, like the ionization chamber, detect star production in the crystal.

3. Crystal counters. These again give a measure of total ionization produced in the crystal and, in general, suffer from the same limitations as the scintillation counter. Brown and Street (8), using a silver chloride crystal, have measured production of stars by charged primaries. Assuming these primaries to be protons, they have found the relative intensity of such star producing protons at 3.4 kilometers and at sea level. Their result checks the more directly measured relative proton rates obtained by Todd (4) using a magnetic cloud chamber technique.

4. Proportional counters. These suffer from the same statistical fluctuations due to knock-on electrons as do the previously mentioned devices. The mechanism of the discharge also gives a large fluctuation in pulse size. The technique can be improved by using a number of such counters in series but still seems incapable of giving good proton-meson analysis.

5. Photographic emulsions. These are mainly useful for measuring relative rates of star production by protons at various altitudes. Although they detect both protons and mesons the scale of events has so far prevented the practical use of emulsions in momentum measurements.

6. Inefficient counters. Counters operated at so low a pressure as to give small efficiencies for detection of minimum ionizing particles can be used in place of proportional counters. A number of such counters would have to be used in series and would suffer from the same statistical fluctuations from knock-on electrons mentioned earlier.

7. Cerenkov radiation counters. Here the principle of operation is different as it does not depend on ionization. As the angle of emission of Cerenkov radiation is a function of the velocity of the particle the technique can be used to measure particle velocities. Because of the small intensity of cosmic radiation, particles must be accepted through a fairly wide angle; thus small velocity differences cannot be detected. However, by using counters and absorbers to define particles in a selected range interval, it should be possible to distinguish between protons and mesons stopping in this range interval. Recent improvements in this technique and in photographic tubes make this an interesting method for future work.

B. Cloud Chamber Techniques

With the possible exception of the Cerenkov radiation counter none of the aforementioned techniques are satisfactory for proton-meson analysis. A simple cloud chamber gives an indication of ionization rates through track density. It does not suffer from the difficulties due to knock-on electrons or failure to distinguish single from multiple events. However, present techniques seem capable of reliably distinguishing only particles of several times minimum ionization from those of minimum ionization, so that the method is limited. The addition of a magnetic field improves one's ability to distinguish between protons and mesons. This technique was used by Potter (3) to show the presence of large numbers of protons in the radiation at 3.4 kilometers. It was later shown that only about one-half of the protons with momentum near 0.5 Bev/c were found in this way, while at higher momenta an even smaller fraction were detected. The more interesting magnetic cloud chamber technique for proton-meson analysis used by Todd (4) will be carefully described in the following paragraph because of its relation to the present work.

C. Magnetic Cloud Chamber Technique Used by Todd (2,4)

In the observations made by Potter a plot of the momentum distribution of particles that were clearly heavily

ionizing showed a sharp cut-off at low momentum. The position of this momentum cut-off, 0.25 Bev/c, corresponded to the momentum of a proton with just enough energy to traverse the absorbing material between the cloud chamber and the Geiger counter used to trigger the chamber expansion. This result suggested the use of a counter-absorber technique to trigger the chamber only for those particles of range in lead greater than some minimum value A but less than some maximum value B. The selection of the values A and B, based on the range momentum relationship for protons and mesons as determined by ionization loss (at equal momenta protons have a smaller range than mesons), could be made so that the protons and mesons recorded would lie in well separated momentum intervals.

The value of A determines the minimum momentum of the protons and mesons recorded. As B is increased the maximum allowed meson momentum approaches the minimum proton momentum. The value of B was chosen as large as possible without leading to overlap of the proton and meson momentum intervals, allowance being made for experimental errors and effects of scattering.

This was accomplished by the experimental arrangements shown schematically in Figure I. The counters C1, C2 and C3 form a triple coincidence telescope. C1 and C2 define a beam of particles through the chamber while C3 requires the

selected particles to traverse the absorber interposed between C2 and C3. The counters A2 in anti-coincidence block the recording of particles traversing it and so require selected particles to stop in the absorber between C3 and A2. Three sets of observations were made with absorber layers as shown in Figure I.

Arrangement A functioned exactly as predicted giving clearly resolved proton and meson peaks as shown in Figure II. For cases B and C the resolution was poor; in fact, it was almost unusable in case C. This poor resolution resulted from combined effects of scattering and proton loss through nuclear interaction in the absorber between C2 and C3. Scattering in the absorber between C2 and C3 resulted in a loss of those particles suffering such deflections as to miss the counter group C3. This scattering required a correction to the observed intensities amounting to 60% of the recorded meson intensity and 30% of the recorded proton intensity for case C. Similarly, scattering in the absorber between C3 and A2 resulted in the erroneous inclusion of particles so scattered as to miss the counter group A2. This caused the inclusion of higher energy mesons that overlapped the recorded protons. A more serious error resulted from loss of protons through nuclear interaction. As was learned later, nuclear interactions lead to a removal path length for protons of about 200 gms/cm^2. The effect here was to reduce

FIGURE 1
EXPERIMENTAL ARRANGEMENT USED BY TODD

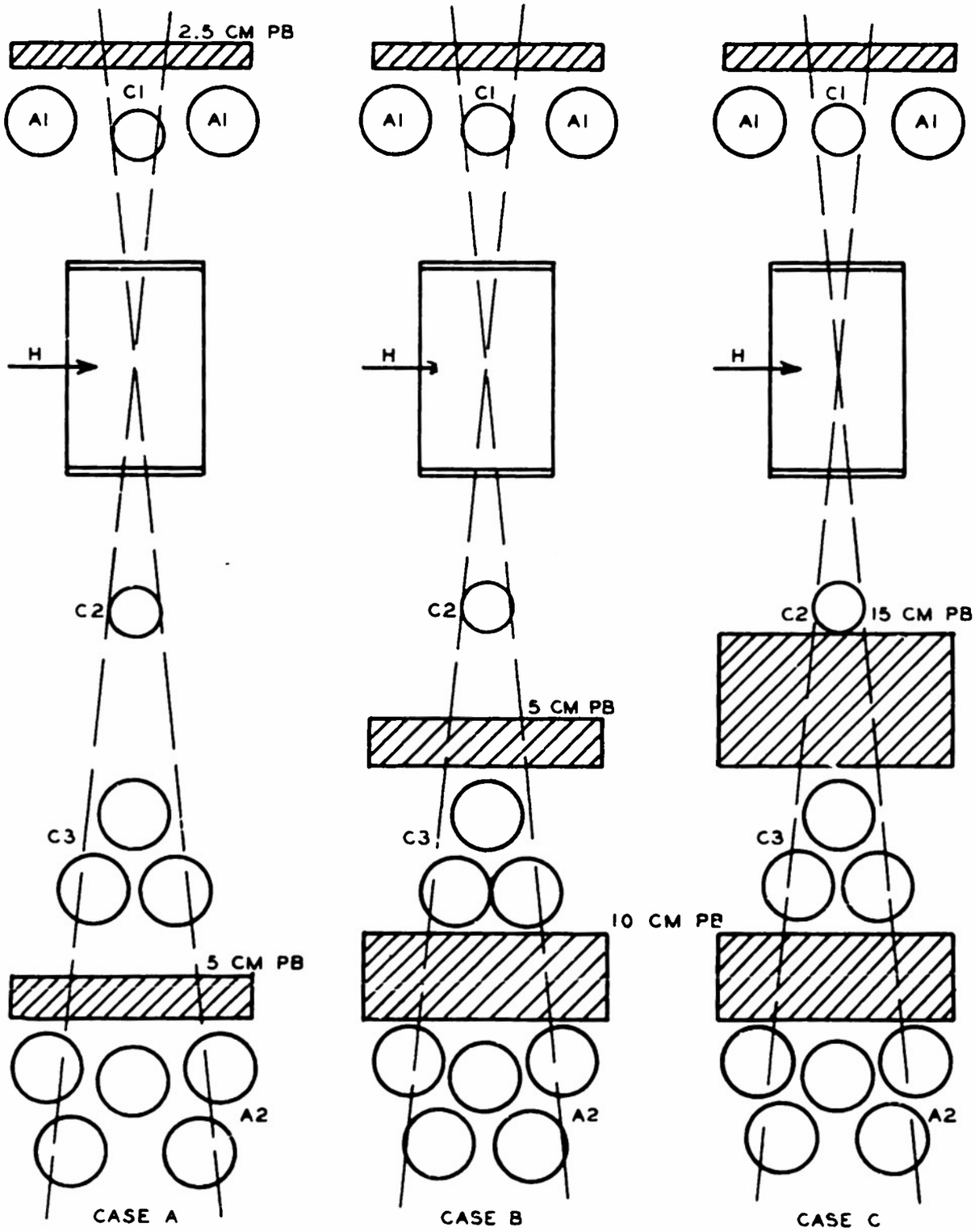

FIGURE 11

MOMENTUM SPECTRA OBTAINED BY TODD

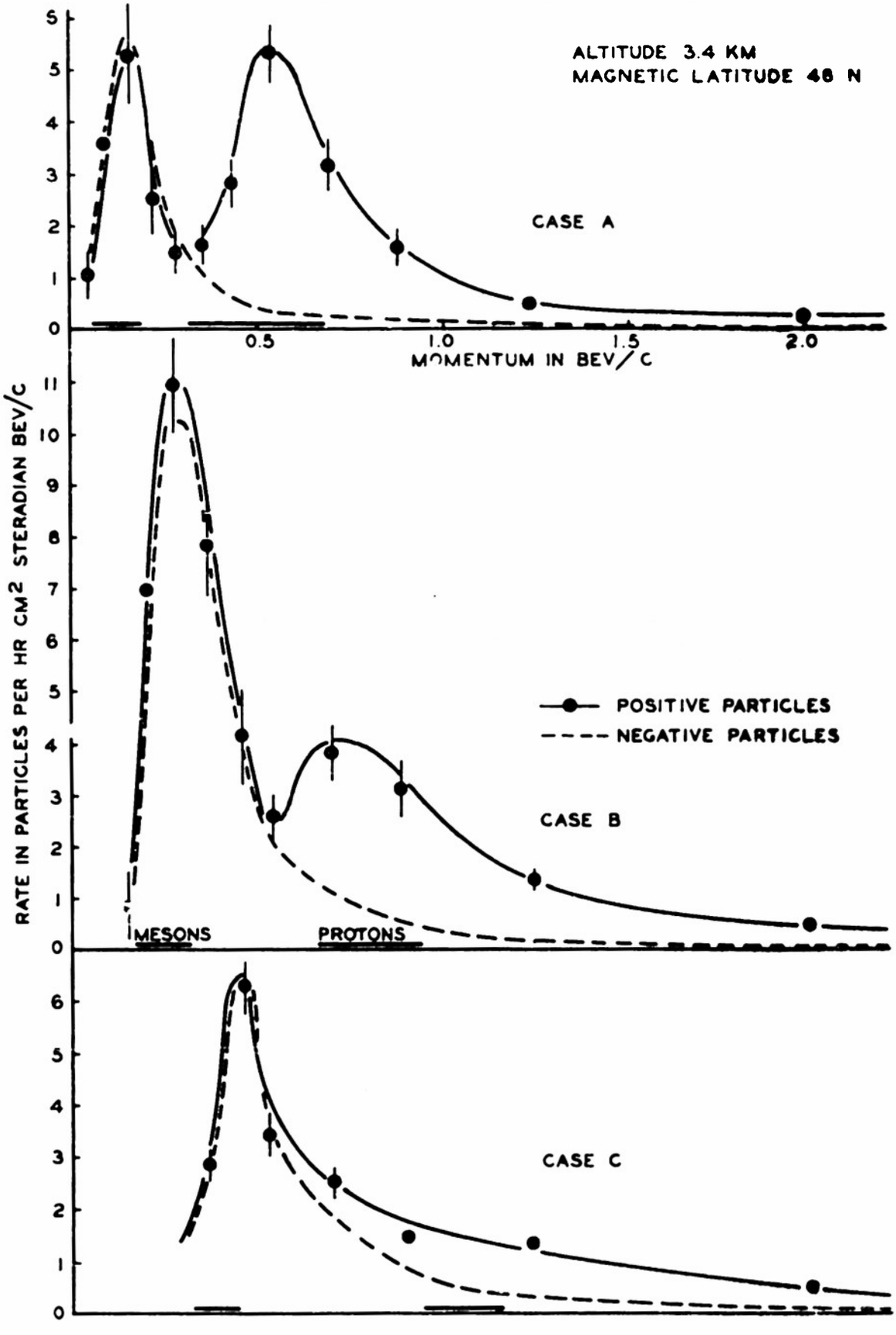

the recorded proton intensity by a factor of about 24% for case B and 56% for case C. For case C so many protons were lost as to invalidate the results. Obviously the technique cannot be extended to the study of proton intensities at higher momenta. Some idea of the overall proton spectrum was obtained by applying the large corrections indicated and combining the results of cases A, B and C.

D. Present Experimental Method

The present experiment is an attempt to overcome the difficulties of the technique discussed in the previous section so as to provide reliable proton intensities at momenta up to about 2 Bev/c. Whereas nuclear loss of protons resulted, in the previous technique, in a serious limitation to the applicability of the method, the present method makes use of this loss in the detection of protons. This is accomplished largely by removing the coincidence counters C3 of Figure I. The telescope is thus reduced to a two-fold coincidence arrangement, C1 and C2. (See Figure III.) The coverage of the anti-coincidence blanking tubes A2 has been greatly extended and large absorber thicknesses (15 and 30 cm) are used between C2 and A2. The minimum range is now reduced to the amount of absorber between the sensitive volume of the chamber and that of the counter C2 (equivalent to about 3.7 gms/cm^2 of lead). The vast majority of particles stopping

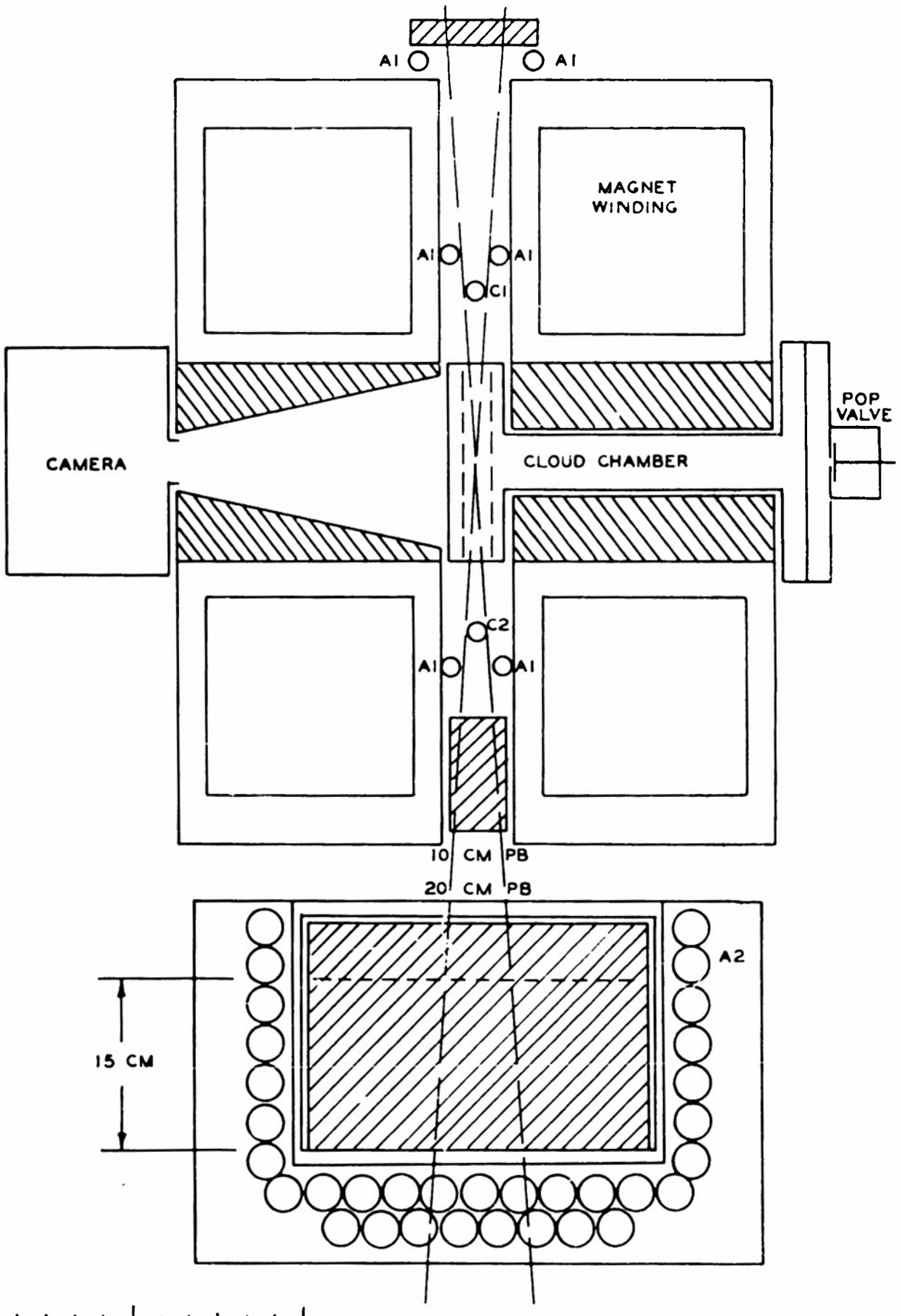

FIGURE III
EXPERIMENTAL ARRANGEMENT

in the large absorber thickness are of sufficiently high momentum to have suffered little scattering between C1 and C2. In addition, as only two-fold coincidence is used, particles scattered in the chamber walls may be scattered either into our out of the coverage of C2. The small number of particles undergoing appreciable scattering, plus the partial compensation as mentioned, make the total effect of scattering in the present arrangement negligible. As shown in Figure III, the A2 coverage has been so extended that particles must be scattered 50 degrees or more in the absorber layer below C2 in order to miss the A2 counters.

Both of the large sources of error present in Todd's observations have thus been eliminated. The minimum range of 3.7 gms/cm^2 of lead is less than 2% of the proton nuclear removal path length, resulting in negligible proton loss in the C-train. As mentioned above, scattering losses in the C-train have also been made negligible. As in Todd's experiment a 2.5 cm lead absorber for electron shower multiplication has been included above C1. This will be discussed later.

The maximum meson momentum, as determined by the total absorber thickness between the chamber and counters A2, is now 0.35 Bev/c in the 15 cm case and 0.57 Bev/c in the 30 cm case. The minimum momentum of protons recorded, as determined by the 3.7 gms/cm^2 load equivalent between the chamber and C2, is 0.28 Bev/c in both cases. Thus, in each case, the

proton and meson momentum intervals slightly overlap. However, since ionization loss causes protons to be included to 1.05 Bev/c for the 15 cm case and to 1.38 Bev/c for the 30 cm case, good proton-meson separation is obtained for both cases above the meson cut-off.

At momenta above the proton ionization cut-off large numbers of protons are still included due to nuclear interactions. For the 30 cm case nuclear absorption of protons is so complete that over 80% are included at the highest momentum measured (2.5 Bev/c). As nuclear absorption is less complete for the 15 cm case, comparison between this and the 30 cm case, as well as with the results of Todd, can be used to compute the nuclear removal path length for protons in lead.

As has been shown previously, and as the results of the present experiment bear out, meson absorption is determined by ionization loss only so that few mesons are included above the meson ionization cut-off (0.35 Bev/c for the 15 cm case) previously mentioned. However, because some are included due to scattering, adequate proton-meson separation is not obtained below about 0.5 Bev/c.

PART III

THE EXPERIMENT

A. Experimental Arrangement

Figure III shows to scale the arrangement of counters and absorbers with respect to the cloud chamber and magnets. Counters C1 and C2 used in coincidence define a beam of particles through the chamber. The six A1 counters all lie outside of, but close to, the coverage defined by counters C1 and C2 and are used in anti-coincidence with these. They serve to reduce the recording of shower-type events. The counters A2, of which there are 33, completely surround a large block of lead absorber so that a charged particle traversing C1 and C2 will not be recorded if it, or one of its charged secondaries, penetrates this absorber. The 2.5 cm of lead absorber above the equipment serves to multiply the density of electron showers penetrating it and thus aid in their recognition through actuation of one of the A1 counters (in which case they are not recorded) or by the appearance of more than one track in the chamber. The function of the lead absorbers between C2 and A2 has been explained. In one series of observations a 30 cm absorber, arranged in two blocks as shown, was used. In another series a 15 cm absorber, placed in the lower position as shown in

the figure, was used.

Since Figure III is drawn to scale the coverage of the anti-coincidence tubes in one plane is easily seen. For the perpendicular plane the lengths and positions of the tubes must be considered. The counters C1 and C2 are each six inches in effective length and are 12 inches apart. The lower layer of A tubes, placed 27 inches below the center of the chamber, would have to have an effective length of 27 inches to provide coverage. Actually the tubes are 30 inches long, but the effective length is only about 27½ inches. Thus about half of those particles accepted at the extreme angle defined by the length of the C counters will be scattered outside the A2 coverage. However, due to geometrical factors, the intensity of accepted particles drops to zero at these extreme angles so that only a small portion of all accepted particles are affected by this. The effect here is to accept some mesons above the computed ionization range where, ideally, protons only would be accepted. This has only the effect of decreasing slightly the statistical accuracy of the determination of the proton intensity near this momentum. For protons the effect is similar in the inclusion of higher energy ones due to scattering. This is not undesirable as the intention of the observations is to include as many protons as possible at all momenta.

The A2 counters are arranged to prevent particle leakage between counters. These are metal-wall counters arranged with adjacent counters in contact. For the bottom layer a second row of counters is used to cover small dead spaces between counters. Along the sides the single rows are considered adequate as very few particles will be so scattered as to traverse these counters and, in addition, they would have to be traveling almost horizontally to pass through the small dead space between adjacent counters.

The principal pieces of experimental equipment, including the chamber, magnet, camera, etc., are the same as those used previously and have been described in detail elsewhere (1,2,3,4). For completeness a brief description is included in the following section.

B. Equipment

1. Magnets. The magnets are wound with 0.25 x 0.80 inch copper strip. A current of 800 amperes provides a field of 8200 gauss and requires about 25 kilowatts of power. The current was continuously recorded and adjusted manually every few hours. Small variations between adjustments of about 1% caused only ½% change in the field, because of near saturation of the magnet, and thus caused no appreciable error.

Cooling is obtained by pumping oil through spaces left between the windings at a rate of 80 gallons per minute. The

oil also passes through a heat exchanger where the heat is transferred to a stream of water which flows constantly through it. The temperature of the oil is automatically held constant by varying the rate of flow through the heat exchanger.

2. Cloud chamber. The cloud chamber is two and one-half inches deep and seven inches in diameter with a useful illuminated depth of one inch. It is filled with a mixture of argon gas and the saturated vapor of a 60-40 n-propyl alcohol-water mixture to a pressure of 1.3 atmospheres. Expansion takes place through a two inch tube ten inches long which extends through the center of one of the magnets. The expansion is produced by the sudden release of air from behind a neoprene diaphram through a pop valve. The tube was filled with copper wool to damp out oscillations.

Tracks are photographed 0.06 seconds after the coincidence pulse through a conical hole in one of the magnets. Stable operation of the chamber requires that the temperature remain nearly constant. An automatic device was used consisting of a copper coil in the oil stream, an a-c bridge, a Brown-type amplifier and a split-phase motor controlling a bypass valve on the heat exchanger. This method provided a constant temperature to about 0.01 degree centigrade.

A clearing field is applied to remove the ions in the chamber before another expansion occurs. This field is automatically removed during the expansion and exposure of

the chamber.

3. Illumination and photography. The cloud chamber was illuminated from the side by means of four Sylvania type R-4340 photo-flash tubes operating at 2500 volts. The flash was provided by the discharge of a 32 microfarad condenser through each tube. An aluminum foil reflector taped part way around each tube and a cylindrical collimating lens aided in projecting the light into the chamber.

The camera used was designed specifically for this equipment. It contains an f4.5 Ektar lens and has a 50 mm focal length. One hundred foot rolls of clear base Linograph Ortho film were used with about 450 pictures per roll. After each exposure the camera automatically wound the film to the next frame. Developing the film with D-19 developer gave a high-contrast fine-grain negative.

4. Geiger tubes. The coincidence tubes were of a type using a glass envelope, a copper cathode, and a 5 mil tungsten wire anode. The cathode is six inches long and three-fourths inches in diameter. The tubes were filled with a mixture of 90% argon and 10% petroleum ether by volume to a pressure such that the tube commenced counting at about 1150 volts. The tubes were operated slightly below the center of the plateau at about 1330 volts.

The anti-coincidence tubes used in the experiment were of a type not previously tried with this apparatus. The previously used glass-walled tubes had the disadvantage of too much ineffective volume due to the glass and the space between the glass and cathode, so that it was difficult to place them so as to give complete anti-coincidence coverage. Metal tubes, however, with the copper cathode as the outer wall, enabled complete coverage with two rows of closely spaced tubes. These were filled and operated in the same manner as the glass tubes. Two sizes were used; one with a diameter of 1¼ inches and 30 inches long, and the other with a diameter of 3/4 inches and 9 inches long.

5. Electronics. Electronic control circuits of largely conventional design perform the various operations necessary for automatic operation of the cloud chamber and associated equipment. A Rossi-type coincidence circuit and anti-coincidence mixer, along with necessary preamplifiers, pulse shapers and pulse generators, provide pulses for events of the types C1 plus C2 minus A1 minus A2 and the type C1 plus C2. Registers record the number of events of both types during any period of operation. The chamber is expanded immediately on receipt of a C-A type pulse and the bank of flash lamps is triggered 0.06 seconds later to allow time for droplet growth. After a short delay the chamber is recompressed, the camera rewound and the expansion circuit sterilized for 90 seconds

to allow the chamber to recover. Unlike most selecting circuits, the A blanking pulse here was arranged to retrigger if a second A count occurred during the blanking pulse from the first one. This eliminates a small source of "leakage" that would occur if a C-A event followed closely an independent A count. Arrangement was made to scale all Geiger tubes during the course of operation in order to detect tube failures.

In addition to the chamber controls, automatic controls of various types maintained constant chamber temperature and backing air pressure, and also provided safety cut-outs to protect the magnets and generators, etc.

C. Experiments Performed

Two sets of observations were made which differed only in the thickness of lead absorber between C2 and the anti-coincidence tubes; 30 cm in one case and 15 cm in the other. They are referred to here as the 30 cm case and tne 15 cm case, respectively.

The equipment was oriented with the chamber axis in a north-south direction. The maximum entrance angle from the vertical for the particles was four degrees to the north and south and 26 degrees to the east and west, resulting in a longer path through the absorber for some of the particles. The effective path length for the measured particles has been calculated to be 3% greater than the thickness of the absorber.

The observations were made at Climax, Colorado, at an elevation of 3.4 kilometers and magnetic latitude 48 degrees north during the summer and fall of 1950. Approximately 6500 pictures were taken for the 30 cm case and 6300 for the 15 cm case.

PART IV

METHOD OF MEASURING TRACK CURVATURE

The equipment used to determine the curvature of the cloud chamber tracks has been described in detail by Potter (3). A brief description is included here.

In general the method consists of enlarging the pictures and comparing them directly with a circular arc of known radius. Thus, from a number of prepared arcs can be selected the one that fits the track best. This was accomplished with a machinist's bench comparator, altered so that a 35 mm photograph could be projected onto a ground glass screen of convenient size. Provision was made for moving the film quickly into position and clamping it in place for proper focus on the screen.

The standard curves were prepared in such a manner that any possible distortion in the optical system was compensated for. An Evans linkage was used to scribe curves of various radii in a layer of Aquadag on a 4 x 7 inch glass plate. A pair of parallel circular arcs 0.7 mm apart made it possible to view the tracks between the arcs instead of tending to obscure a track by placing a single arc over it. The scribed plates were photographed with the same camera and at the same distance used in photographing cloud chamber tracks. Thus

optical distortions were the same for cloud chamber tracks as for the standard arc, making it unnecessary to know the magnification of the projecting system. These photographs were placed in the comparator so that the curves were projected onto the ground glass screen. The screen was replaced by a 2½ x 7 inch Kodak 33 plate which, after exposure, was used to make a positive on a similar plate. The result was a 2½ x 7 inch glass plate with six pairs of curves, each with a slightly different radius. Four such plates with curves designated A to X made up a set which enabled measurement of tracks with radii between 0.3 and 10 meters.

PART V

METHOD OF DETERMINING RATES

Not all of the photographs taken show single proton or meson tracks. Some show showers while others fail to show any track and are referred to as misses. The occurrence of events of these types will be discussed in Part VIII. Only single tracks were measured and used for determining rates. In addition, only those tracks of length at least 88% of the chamber diameter were measured. Shorter tracks were not used because they cannot be measured as accurately and their position nearer the chamber wall leads to greater track distortion. With the exception of tracks whose widths indicated that they were not time coincident with the triggering pulse, all single tracks of the necessary length were included regardless of quality or track density.

Our problem then is to determine, from the measurements of the tracks thus selected, the absolute proton and meson rates at a given momentum. This is accomplished by assuming that the proton plus meson rate is proportional to the C-A counting rate and to the percentage yield of all single tracks regardless of length. The assumption is also made that the momentum distribution of the particles is the same as for the tracks of the required length. This involves only the natural assumptions that track selection by length does

not discriminate according to momentum and that the distribution of events photographed is the same as the distribution among all events producing C-A counts. (The number of C-A events and photographs does not correspond because of chamber sterilization during recovery time.)

The single track rate, STR, can be obtained from the C-A rate by knowing the fraction of the C-A counts that result in a single track. This fraction is just the ratio of all single tracks, including those too short to measure, to the total number of frames examined. Thus

$$\text{STR} = \frac{\text{Single Tracks}}{\text{Total Frames}} \text{ (C-A rate)} \qquad (1)$$

To obtain the rate for some N measured tracks in a momentum interval dp, the STR must be multiplied by the ratio of N to the total number of measured tracks, M. If the acceptance of the counter telescope is S cm^2 steradians then the absolute rate is given by

$$\text{Rate} = \frac{1}{S} \frac{1}{dp} \frac{N}{M} \qquad (2)$$

in particles per hour cm^2 steradian Bev/c.

From the geometry of the telescope S was measured as approximately 1.0 cm^2 steradian. This measurement cannot be made accurately because of uncertainty as to the effective size of the Geiger tubes. However, earlier measurements with the same coincidence arrangement gave rates (computed with

this value of S) that agree well with values given by Rossi (9), Greissen (10) and others so that the value 1.0 cm^2 steradian was assumed to give proper normalization.

For convenience the quantities in the above equation that are constant for each case are grouped together to form a "normalization factor" given by

$$NF = \frac{STR}{M}. \tag{3}$$

Using this quantity the rates are quickly computed from the formula

$$Rate = \frac{N}{dp}\,(NF). \tag{4}$$

PART VI

DATA

Table I is a tabulation of the curvature measurements for the two cases. Each singly occurring track longer than 15 cm was measured in the comparator and its curvature recorded as either equal to one of the curves A to X or midway between two curves. A few tracks with curvature greater than A or less than X were also recorded.

Table I also shows the number of tracks in each interval judged to be heavily ionizing. These tracks were selected by examining the photographs in a viewer, in which ten frames at a time were presented, and selecting those tracks that seemed to be appreciably denser than the average for the group of frames. It is not suggested that these either represent all protons or are exclusively protons as will be discussed later.

Tables II and III contain a summary of the analysis of each case. Here the particles have been grouped into larger intervals, as shown, to improve the statistics. Non-overlapping intervals were used. The momentum for the center of the interval and the interval width in Bev/c is given in each case. By the method of normalization previously explained the absolute rate in particles per hour cm^2 steradian Bev/c has been computed for each interval. All

information from examination of the photographs that is necessary for rate determination has been included. By straight tracks is meant those meeting the imposed length requirement but of too large momentum to permit measurement. In Figures IV and V have been plotted the rates as given in Tables II and III for positive and negative particles and for those judged as heavily ionizing.

TABLE I - MEASUREMENT OF TRACK CURVATURES

Interval	Radius Meters	Number of Tracks Measured 15 cm Case Pos.	Neg.	Heavy	30 cm Case Pos.	Neg.	Heavy
		23	23		24	26	
A	0.316	19	22		10	17	
		8	7		4	5	
B	0.400	19	31		22	16	
		12	6		3	6	
C	0.515	29	20		14	19	
		1	3		2	1	
D	0.583	27	18		16	21	
		1	3		7	2	
E	0.661	22	23		21	15	
		2	8		4	3	
F	0.751	21	27		29	19	
		7	9		11	4	
G	0.852	31	51		30	32	
		10	11		10	5	
H	0.966	49	46	1	37	40	
		13	7		9	8	
I	1.09	77	52	1	49	40	3
		18	8		14	8	
J	1.23	91	54	25	48	49	9
		15	13		11	10	
K	1.39	64	50	20	65	51	20
		17	13		14	13	
L	1.56	53	30	27	58	43	29
		9	5		24	17	
M	1.74	44	13	36	115	68	30
		11	2		20	21	
N	1.94	48	10	42	103	57	51
		13	2		31	16	
O	2.16	59	5	39	109	68	44
		21	1		28	9	
P	2.42	67	8	52	78	39	45
		23	4		35	11	
Q	2.73	66	1	43	56	26	37
		23	1		15	2	
R	3.08	81	4	35	83	15	30
		29	2		23	3	
S	3.51	79	5	33	95	14	19
		25	1		25	4	
T	4.06	78	4	21	68	8	19
		13	0		20	1	
U	4.81	50	4	16	67	7	10
		15	0		11	3	
V	5.85	62	4	4	75	8	5
		6	0		4	1	
W	7.41	56	11		59	7	
		8	1		4	0	
X	10.00	70	7		79	13	
		103	24		108	20	

TABLE II

30 CM CASE

Climax, Colorado
Elevation 3.4 km

September 1950

Track Measurements

Positives	1846	Average single track yield	62.2%
Negatives	892	C-A rate per hour	29.8
Straight tracks	32	Single track rate	18.5
Total measured	2770	Normalization factor	.00668
Short tracks	1287	Film numbers	C1 to C16
Showers	763		
Misses	1718		
Total frames	6538		

Interval	Momentum at Center Bev/c	Momentum Interval Bev/c	Number of Particles Positive	Negative	Heavy
To A	0.05	0.079	29	34	
A-E	0.123	0.863	83	86	
E-I	0.220	0.107	166	138	
I-L	0.333	0.117	205	173	45
L-N	0.438	0.095	240	156	70
N-P	0.545	0.120	258	141	92
P-R	0.688	0.165	187	66	74
R-T	0.893	0.245	218	33	44
T-V	1.24	0.448	170	19	22
V-X	1.98	1.038	144	18	
X-on			148	26	

Interval	Rates Positive	Negative	Difference Pos. and Neg.	Heavy Track Rate
To A	2.5 ± .5	2.9 ± .5		
A-E	6.5 .7	6.7 .7		
E-I	10.3 .8	8.6 .7	1.7 + 1.1	
I-L	11.8 .8	9.8 .8	2.0 1.1	2.6 ± .4
L-N	16.8 1.1	11.0 .9	5.8 1.5	4.9 .6
N-P	14.4 .9	7.8 .7	6.6 1.1	5.1 .5
P-R	7.6 .5	2.7 .3	4.9 .6	3.0 .4
R-T	6.0 .4	.9 .2	5.1 .5	1.2 .2
T-V	2.5 .2	.3 .1	2.2 .2	.3 .1
V- X	.9 .1	.1 .03	.8 .1	
X-on				

TABLE III

15 CM CASE

Climax, Colorado
Elevation 3.4 km

October 1950

Track Measurements

Positives	1688	Average single track yield	53.0%
Negatives	654	C-A rate per hour	21.8
Straight tracks	25	Single track rate	11.5
Total measured	2367	Normalization factor	.00488
Short tracks	980	Film numbers	D1 to D15
Showers	916		
Misses	2062		
Total frames	6325		

Interval	Momentum at Center Bev/c	Momentum Interval Bev/c	Number of Particles Positive	Negative	Heavy
To A	0.050	0.079	32	34	
A-E	0.123	0.863	117	110	
E-I	0.220	0.107	182	196	
I-L	0.333	0.117	270	179	61
L-N	0.438	0.095	114	40	71
N-P	0.545	0.120	150	17	86
P-R	0.688	0.165	186	12	87
R-T	0.893	0.245	212	12	61
T-V	1.24	0.448	148	8	28
V-X	1.98	1.038	136	17	
X-on			138	27	

Interval	Rates Positive	Negative	Difference Pos. and Neg.	Heavy Track Rate
To A	2.0 ± .4	2.1 ± .4		
A-E	6.6 .6	6.2 .6		
E-I	8.4 .6	9.1 .7		
I-L	11.7 .7	7.4 .5	4.3 ± .8	2.5 ± .3
L-N	5.9 .6	2.1 .3	3.8 .7	3.6 .4
N-P	6.1 .5	0.7 .2	5.4 .5	3.5 .4
P-R	5.5 .4	0.4 .1	5.1 .4	2.6 .3
R-T	4.2 .3	0.2	4.0 .3	1.2 .2
T-V	1.6 .1	0.1	1.5 .1	0.3 .1
V-X	0.6 .05	0.1	0.5	
X-on				

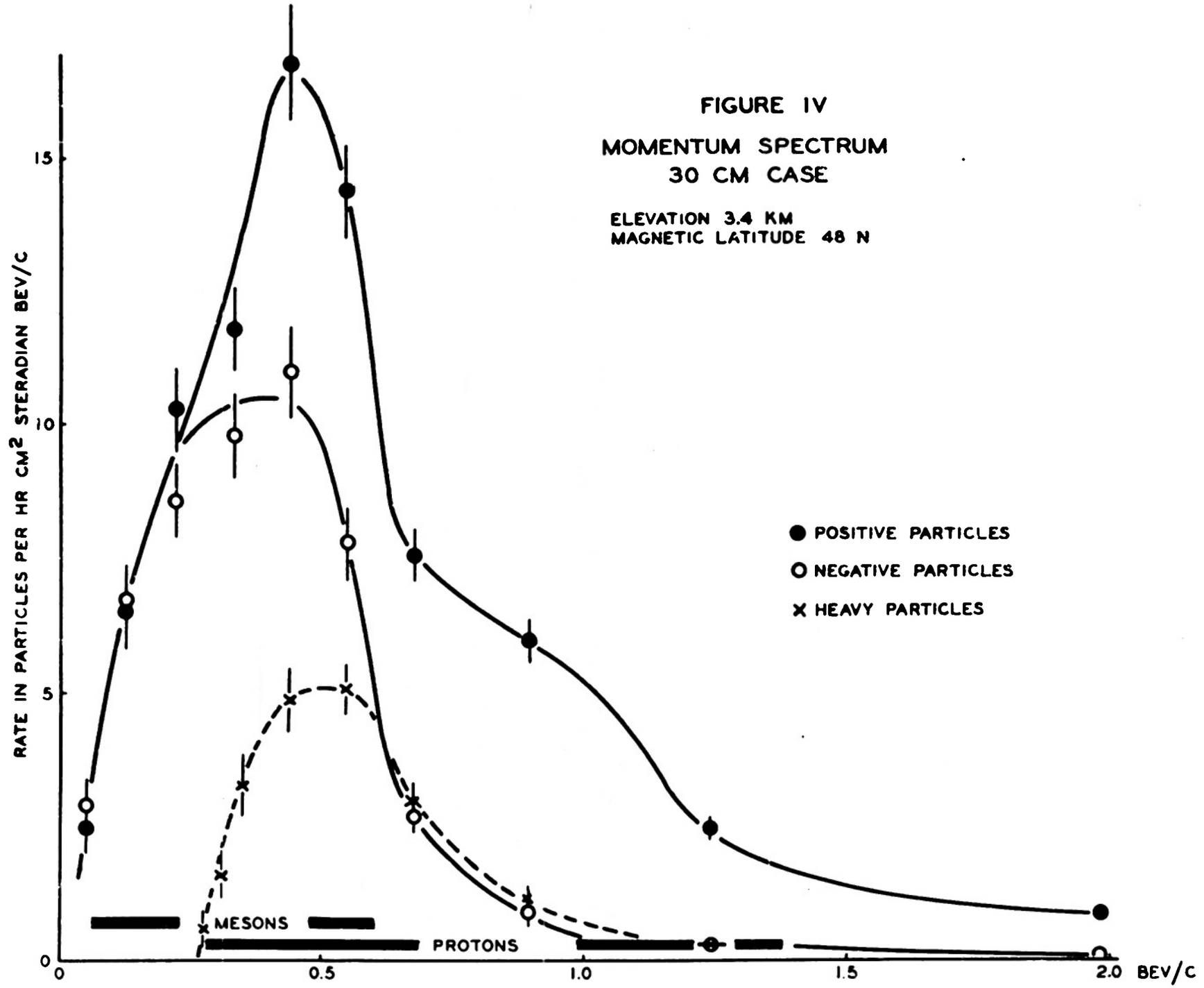
FIGURE IV
MOMENTUM SPECTRUM
30 CM CASE
ELEVATION 3.4 KM
MAGNETIC LATITUDE 48 N
POSITIVE PARTICLES
NEGATIVE PARTICLES
HEAVY PARTICLES
RATE IN PARTICLES PER HR CM2 STERADIAN BEV/C
15
10
5
0
0
0.5
1.0
1.5
2.0 BEV/C
MESONS
PROTONS

FIGURE V

MOMENTUM SPECTRUM
15 CM CASE

ELEVATION 3.4 KM
MAGNETIC LATITUDE 48 N

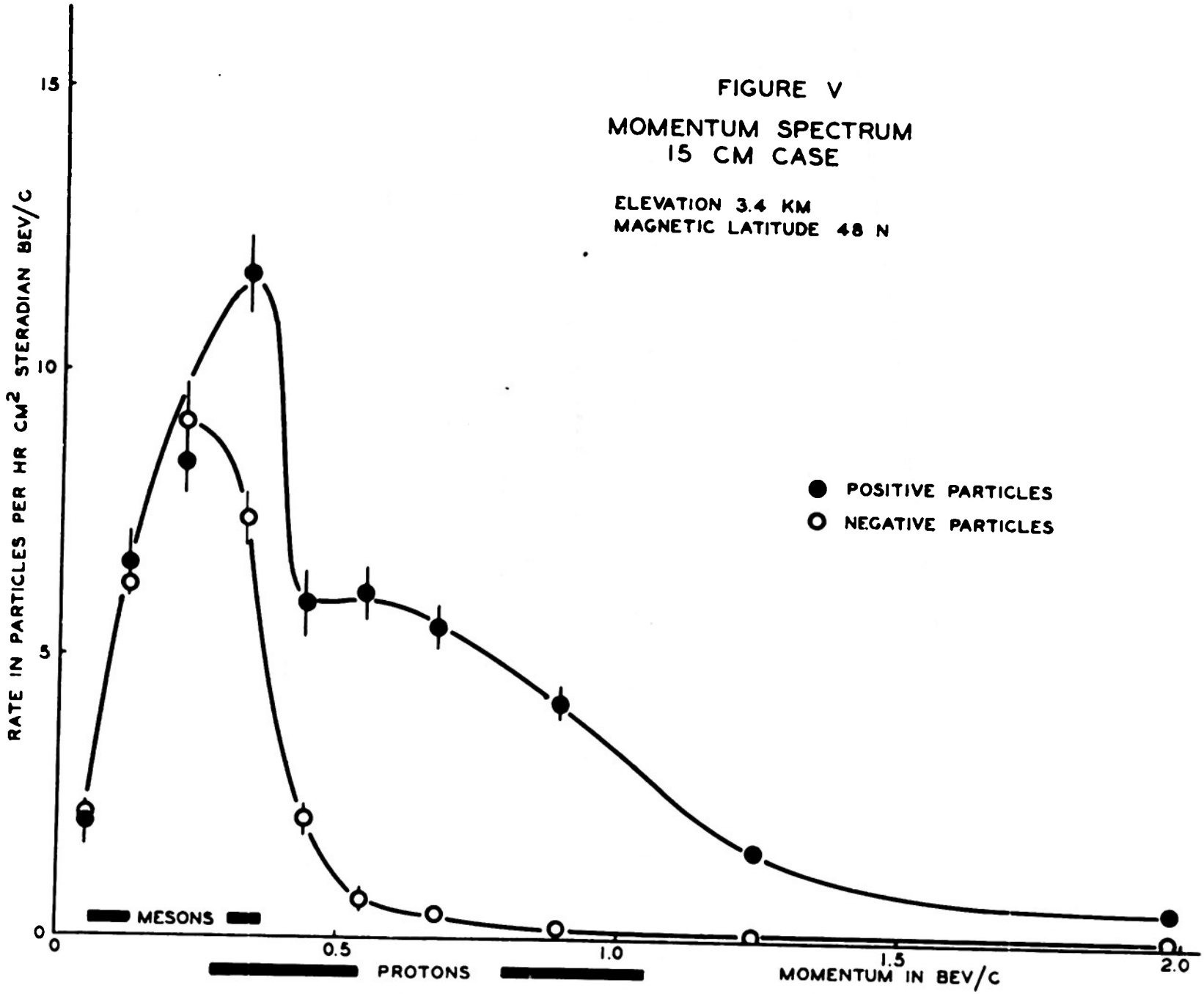

PART VII

RESULTS AND DISCUSSION

Part VII contains four sections, each of which presents a separate topic, and a final section to compare the results obtained with those of other investigators. Section A is concerned with the details of the graphs of the momentum spectra for all particles recorded, including the selected heavily ionizing particles. The interpretation of the graphs is given along with an explanation of the methods used to identify various components of the radiation. In Section B the proton component is separated from the other radiation to give the momentum spectrum from 0.7 to 2.0 Bev/c.

Section C contains the calculation of the mean free path for removal of protons in lead by nuclear interaction. This quantity is referred to hereafter by the symbol L. In Section D the positive excess for mesons alone is determined. Section E compares the results obtained here with all similar work published to date.

A. Momentum Distribution

In Figures IV and V are given the distributions, according to momentum, of singly occurring particles as selected by the experimental arrangement used. From the

design of the experiment these should represent the momentum spectra of charged particles other than electrons at an altitude of 3.4 kilometers and magnetic latitude 48 degrees north which have ranges in lead from 3.7 to 388 gms/cm^2 and from 3.7 to 2.0 gms/cm^2, respectively. These, of course, do not include all charged particles at this altitude. Indeed, the vast majority of mesons at this altitude have ranges in excess of the upper limits imposed here, as shown by previous work (3) in which the total spectrum was obtained. For protons, however, the 30 cm case should include almost all of those present in the radiation and having momenta above 0.3 Bev/c. The determination of this proton intensity is the primary objective of this experiment.

At the bottom of each figure is indicated the momentum interval for mesons and protons corresponding to the ranges in lead as imposed by the experiment. These have been taken from the range values given by E. P. Gross (11). The ranges are based on energy loss through ionization only and are not expected to be correct for protons which undergo occasional catastrophic losses through nuclear interaction. Mesons are known to have nuclear interaction path lengths (at least 1000 meters) in lead many times longer than the absorber thicknesses used here so that the indicated ranges for these particles are expected to be correct.

The particles included in the distribution are believed to be only mu mesons and protons with the exception (at low momenta) of a number of electrons too small to affect the observed values within statistics. This small electron contamination will be discussed in Section VIII, Errors and Criticisms. The spectra of negative particles are then for mesons only while the positive spectra are for positive mesons plus protons. The decided difference between the positive and negative distributions for the two cases is an indication of the magnitude of the proton intensity. This difference would exactly represent the proton intensity if positive and negative mesons occurred in equal numbers. From many investigations (12-17) the positive meson intensity is known to exceed that of the negatives by some 20%.

Failure of the negative distribution to drop more sharply above the meson cut-off is attributed, in part, to scattering outside the A2 coverage. As indicated earlier, sufficient A protection was not provided in the long dimension of the beam cross-section defined by the coincidence telescope. It is due also to the limited momentum resolution that results from grouping the particles into the rather wide momentum intervals needed to keep the statistical errors small. This is particularly evident for the 30 cm case where the intensity at 0.7 Bev/c is the average intensity for an interval of 0.165 Bev/c. Inclusion of these high energy

mesons above the cut-off has only the effect of adding some statistical uncertainty to the proton intensity determination. The difficulty is avoided in the 15 cm case by using no measurements below 0.5 Bev/c in determining the proton intensity.

Figure IV shows, in addition to the distribution of total positives and negatives, the momenta of those tracks selected as having greater than minimum density. These tracks were selected without regard to sign of curvature. Of the 351 tracks so selected for the 30 cm case, one with momentum 0.54 Bev/c showed negative curvature. Of the corresponding 395 tracks for the 15 cm case, two with momenta 0.35 Bev/c were of negative curvature. Among all tracks judged as heavily ionizing, this 0.4% showing negative curvature probably represents protons back-scattered from the absorber below the C-train. A similar small percentage of such tracks was found in earlier work (3). The intensities shown for these heavily ionizing tracks may not represent true proton intensities as their determination is based, in part, on one's ability to recognize these tracks. At a momentum of 0.5 Bev/c protons have an ionization density of three times minimum; and this density increases rapidly at lower momentum where it is probable that most protons have been found in this way. Indeed, here the intensity of heavily ionizing tracks accounts for most of the difference in

intensity between total positives and negatives. At 0.75 Bev/c protons have an ionization intensity of two times minimum. At this and higher momenta few of the protons present are recognized through track density as will be seen by comparison with the total proton intensity, discussed in the following section.

As is expected from the experimental arrangement, the distribution of heavy tracks shows a sharp cut-off on the low momentum side. For the 30 cm case (Table I) three heavy tracks were found with momentum near 0.28 Bev/c while none were found at lower momenta. The distribution of Figure IV is drawn to zero at this value. Similarly for the 15 cm case, a heavy track was found at both 0.25 and 0.28 Bev/c with none at lower momenta. These experimental cut-offs correspond satisfactorily with that for protons as computed from the minimum range for the experiment.

B. Proton Spectrum

The problem now is to combine all available data to give a best estimate of the proton spectrum at Climax. This is obtained in part from the difference between the positive and negative intensities, and in part (at momenta below 0.5 Bev/c) from the intensity of heavily ionizing tracks. At momenta above 1.0 Bev/c a small correction involving a knowledge of the nuclear removal path length is necessary.

This path length is estimated and discussed in the next section. For comparison, data from earlier work (4), in which particles stopping in 5 cm of lead were studied, are included.

Tables II and III give the difference between the positive and negative rates for each interval. These have been plotted in Figure VI separately for the 15 and 30 cm cases. For the 15 cm case only those positive-negative differences above 0.5 Bev/c are included. At lower momenta the increasing meson intensity makes the magnitude of the difference uncertain and a correction would have had to be made for the positive meson excess. Similarly for the 30 cm case only differences above 0.65 Bev/c are included. The intensities plotted at 0.33 and 0.45 Bev/c are taken from the heavy track distributions which probably give a better estimate of the proton intensity at these momenta than is given by the positive-negative difference. Also included in Figure VI are similar values from earlier work with 5 cm of absorber.

The agreement of Figure VI between the maximum intensities for the various cases is considered satisfactory. For the 15 and 30 cm cases the peak intensities agree well within the indicated statistics. For the 5 cm case the peak intensity is somewhat low. Here the sharp maximum (corresponding to the small absorption range used) cannot be expected to be properly resolved without obtaining intensities at more

FIGURE VI

MOMENTUM SPECTUM
PROTONS STOPPED IN ABSORBER

ELEVATION 3.4 KM
MAGNETIC LATITUDE 48 N

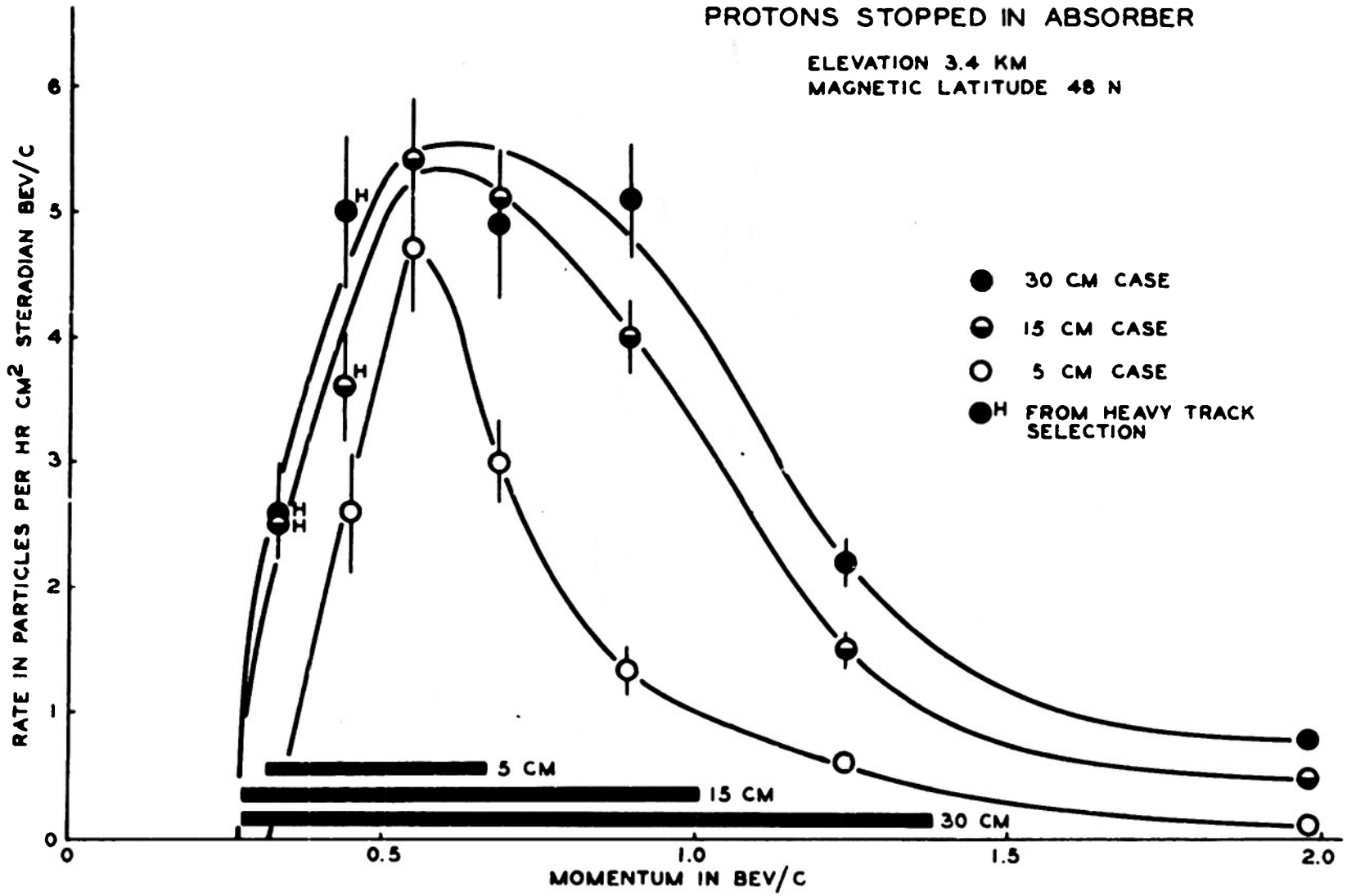

closely spaced intervals. Also, as explained earlier, the arrangement of counters and absorbers used here led to errors of scattering not present in the present observations. For all three cases in Figure VI the low momentum cut-off is an instrumental effect and occurs at the same momentum since the minimum ranges selected were the same.

The intensities at high momenta in Figure VI increase successively from the 5 to the 30 cm case as is to be expected. The small increase from 15 to 30 cm shows that the intensity obtained with an infinite absorber thickness would not be much larger, i.e. almost all protons at these momenta stop in 30 cm of lead.

Figure VII gives total proton intensities as computed from the three distributions of Figure VI. To some extent the intensities of Figure VII need to be discussed point by point. The intensities for each case lying well within the interval for proton stopping through ionization have been transcribed without change. For the 5 cm case the intensities at 0.45 and 0.70 Bev/c have been omitted as uncertain due to scattering as explained earlier. For each case, intensities well above the ionization cut-off have been corrected to total intensities assuming a nuclear removal path length of 206 g/cm^2. The method of doing this will be explained in the next section. The points in Figure VII show some spread, but since they come from different sets

FIGURE VII

MOMENTUM SPECTRUM OF PROTONS
UNDER 2.5 CM OF LEAD

ELEVATION 3.4 KM
MAGNETIC LATITUDE 48 N

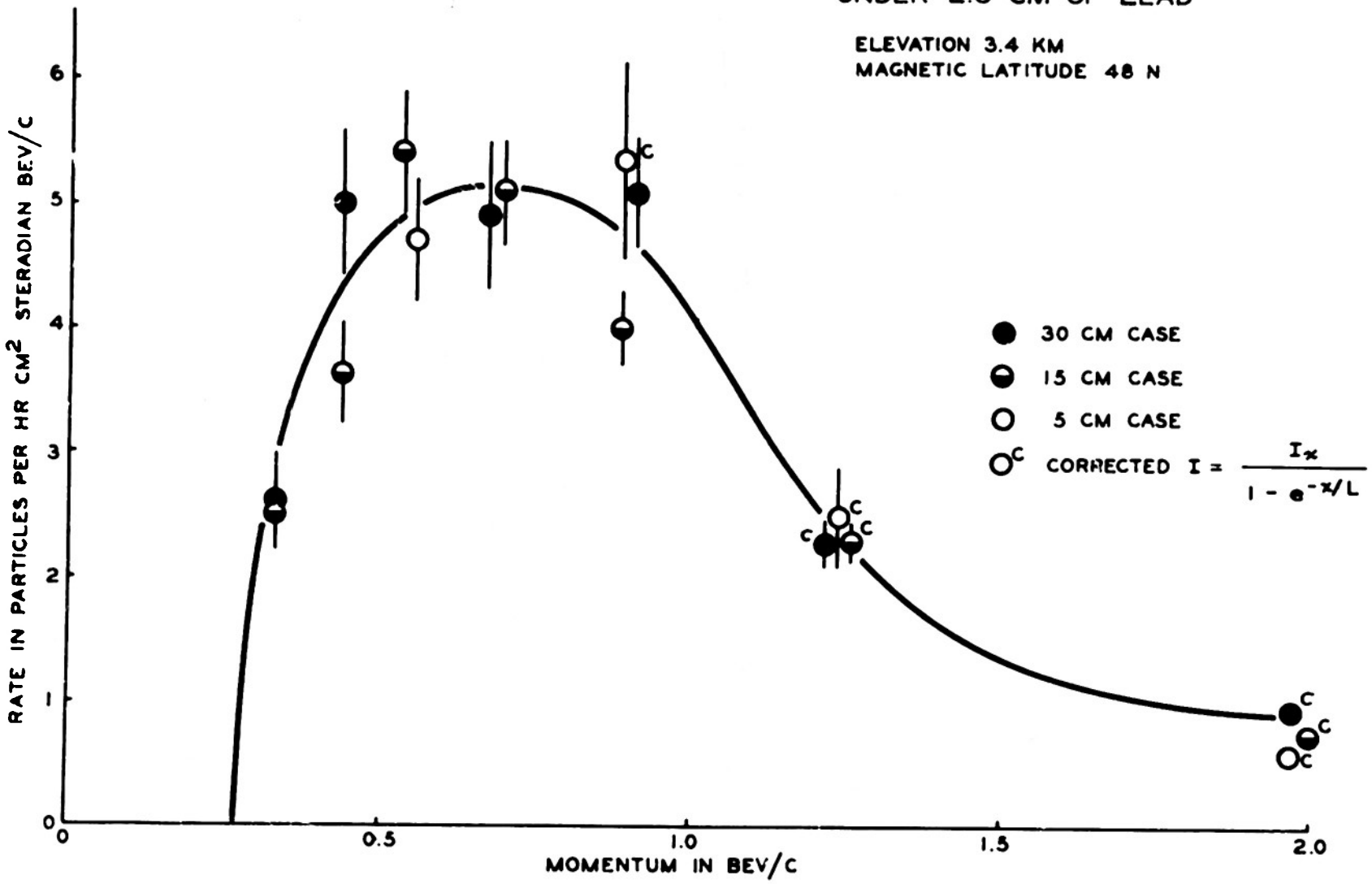

of observations and have rather large statistical uncertainties, the agreement among the various estimates is considered quite good.

In Figure VIII the various estimates of intensity have been combined to give a single value at each momentum. The intensities of Figure VII are all for the radiation as observed under the 2.5 cm lead absorber used above the chamber. In Figure VIII a correction has been made for this, for the counter C1, the top of the chamber, and the roof of the trailer, assuming the path length as mentioned above. This amounts to multiplying each intensity of Figure VII by 1.21 and plotting the result at the momentum the protons would have had before entering the lead. The difference in shape, as well as the higher momentum cut-off, of Figure VIII as compared to Figure VII is due to this correction. Figure VIII, then, is expected to give the atmospheric intensities of protons at the altitude 3.4 kilometers between momenta of 0.7 and 2.0 Bev/c. The rapid decrease in intensity below 0.7 Bev/c is, of course, experimental. In any case, the actual intensity must fall rapidly at low momentum as protons of momenta 0.2 Bev/c, for example, have a range of air at this altitude of only two meters.

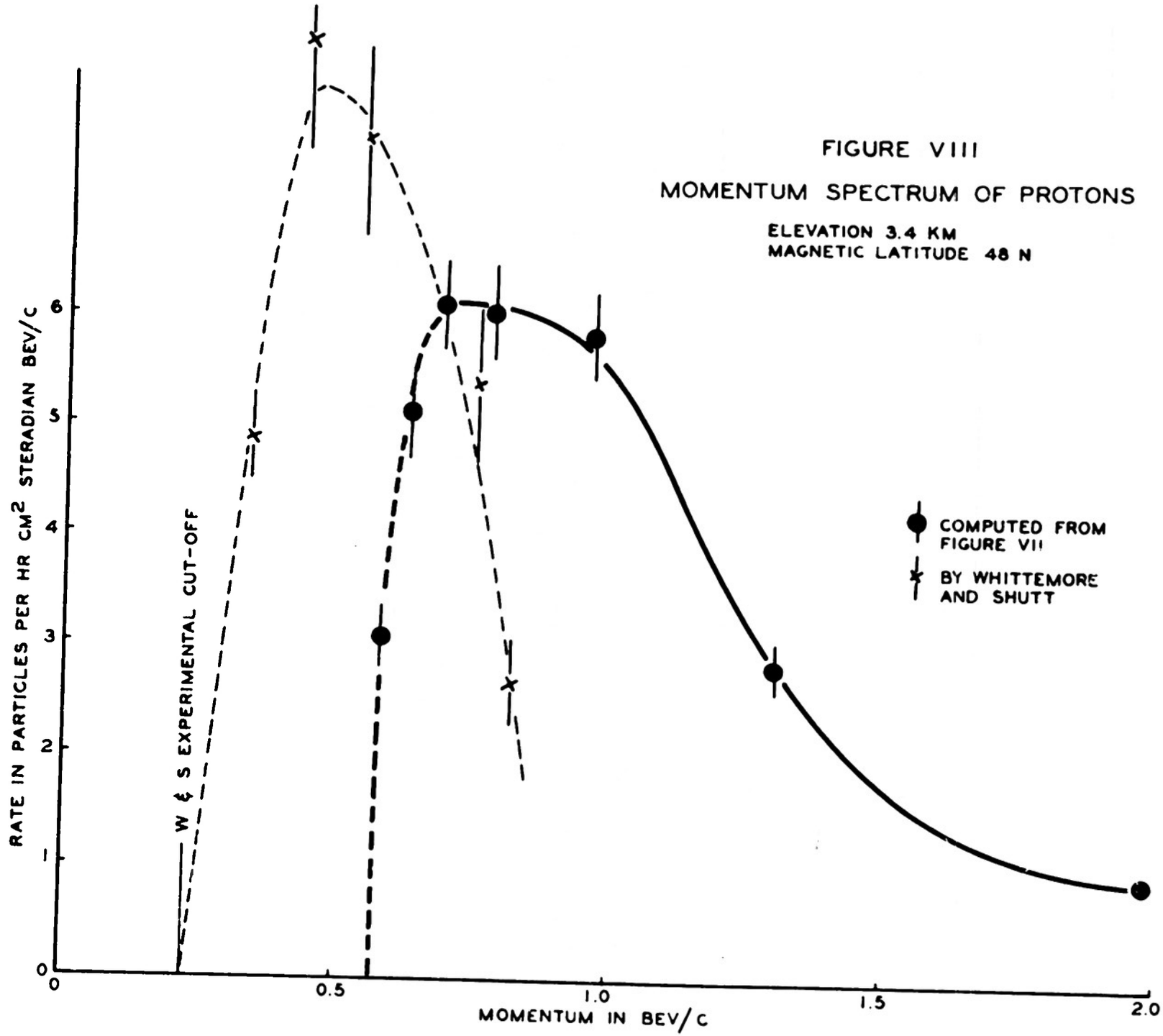
FIGURE VIII
MOMENTUM SPECTRUM OF PROTONS
ELEVATION 3.4 KM
MAGNETIC LATITUDE 48 N
COMPUTED FROM FIGURE VII
BY WHITTEMORE AND SHUTT
W & S EXPERIMENTAL CUT-OFF
RATE IN PARTICLES PER HR CM2 STERADIAN BEV/C
MOMENTUM IN BEV/C
0
0.5
1.0
1.5
2.0
1
2
3
4
5
6

C. Nuclear Interactions of Protons in Lead

In addition to the loss of energy due to ionization, protons occasionally suffer catastrophic losses by collisions with nuclei. The result of the collision may be a scattering of the proton or a disruption of the nucleus with the emission of a number of secondary particles. In the case of scattering the scattered direction may be such that the extended path through the absorber is so much longer than the vertical thickness that particles may stop in the absorber even though they have sufficient energy to traverse vertically through the absorber. In the case of a nuclear disruption a secondary may have sufficient energy to penetrate the remainder of the absorber. The removal of protons as a result of such collisions is usually described by assuming that the intensity at x cm of absorber is given by

$$N_o - N_x = N_o e^{-x/L} \qquad (5)$$

where N_o is the number of protons incident on the absorber, Nx is the number stopping in x cm of absorber due to nuclear interactions, and L is the mean free path for removal of the protons. L, of course, differs from the nuclear interaction mean free path only because of an occasional interaction that either causes so little change in the direction and energy of the incident proton that the proton continues

through the absorber or else produces a secondary that penetrates the remaining absorber.

Calculation of L can be conveniently made from a measurement of the protons stopped by nuclear interaction along with a corresponding measurement of the total intensity of protons incident on the absorber. Examination of Figure VI shows that, for the 30 cm case, there is a large momentum interval where protons would be stopped by ionization losses alone. Since 30 cm is expected to be considerably greater than L, most of the protons at higher momenta will be stopped due to nuclear interaction. Thus, the interval 0.8 to 2.5 Bev/c contains nearly all the protons incident on the absorber.

For the 15 cm case the region from 1.2 to 2.5 Bev/c was selected as one in which the intensity represents protons stopped only by nuclear interaction. This intensity is compared to the corresponding intensity for the 30 cm case, which is assumed to give the total intensity, in arriving at an approximate value for L. Since the 30 cm intensity at high momenta is not quite as large as the total intensity, this approximate value is then used in obtaining a second approximation.

It is not immediately evident that, at 1.2 Bev/c for the 15 cm case, the effect of scattering is not present. However, from range versus momentum curves (11) it can be determined that a 1.2 Bev/c proton would have, after

penetrating the 15 cm absorber, a residual momentum of 0.78 Bev/c. Similarly, a 1.05 Bev/c meson would have 0.78 Bev/c momentum after penetrating the absorber. Multiple scattering from coulombic interaction is determined by the magnitude of p v/c, where p is the momentum of the particle. In the case above, the proton has somewhat higher average momentum in the absorber but smaller v/c than the meson so that the average values of p v/c are equal. Thus, multiple coulombic scattering should be the same for a 1.2 Bev/c proton and a 1.05 Bev/c meson in penetrating the 15 cm of lead. Mesons are known to show coulombic interaction only. The negative meson intensity at 1.0 Bev/c for the 15 cm case (see Figure V) is only 2% of the total negative intensity at this momentum. Actually the appearance of even this small number of mesons at this momentum has later been shown to be due to A-counter dead time rather than scattering. Thus, no appreciable fraction of protons of 1.2 Bev/c momentum are expected to be photographed as a result of coulombic scattering. Of course, large angle single scattering from nuclear interaction may result in a longer path length so that the proton will stop or be scattered outside the A coverage. The effects of such nuclear scattering are included in the definition of L.

For the 5 cm case a similar computation shows that, at 0.8 Bev/c, the effect of scattering is negligible. The

interval chosen for the computation of L is 0.8 to 1.3 Bev/c. The intensity here is compared with the total intensity for this interval as given by the 30 cm case. Extending the interval to higher momenta would have increased the number of particles included in the protons stopped in 5 cm of absorber, but at higher momenta a correction to the 30 cm intensity would have to be made to obtain the total intensity, thus no advantage would be gained. Also, the use of 30 cm data in an interval other than that used in the previous calculation makes the two calculations independent.

Table IV contains the two separate calculations of L, along with statistical errors, and the average of the two results. Since the 5 cm case involved a 3-fold coincidence, it was necessary to correct for the protons lost between C2 and C3. This was done by using an estimated value for L to compute the number lost. The result obtained is 206 ± 30 g/cm^2.

Calculation of L from a comparison of the 5 and 15 cm cases cannot be made with an accuracy comparable to those of Table IV. This results from the inability to determine the shape of an exponential curve from two points on the fairly straight part of the curve.

In Figure VI the values at higher momenta for the 5 and 15 cm cases represent the number that are removed by nuclear interactions in the absorber. Using the value of

TABLE IV

CALCULATION OF L

Case	Momentum Interval	Particles Pos.	Neg.	Difference	Normalization Factor	Rate
5 cm	0.82-1.33	61	4	57	.0318	1.81 (1.87)*
30 cm	"	297	37	255	.0267	6.81
15 cm	1.20-2.50	207	22	185	.0195	3.61
30 cm	"	226	29	197 (219)**	.0267	5.85

Cases	N_o-N_x	N_o/N_o-N_x	ln N_o/N_o-N_x	x	L
5 & 30	4.94	1.38	0.322	62.4	194 $\pm$ 37
15 & 30	2.24	2.61	0.96	207	221 $\pm$ 41
				Average L	206 $\pm$ 30

$$\epsilon^2(L) = \left(\frac{\partial L}{\partial N_o}\right)^2 \epsilon^2(N_o) + \left(\frac{\partial L}{\partial N_x}\right)^2 \epsilon^2(N_x)$$

$$\bar{L} = \frac{\frac{L_1}{\epsilon_1^2} + \frac{L_2}{\epsilon_2^2}}{\frac{1}{\epsilon_1^2} + \frac{1}{\epsilon_2^2}}, \quad \epsilon(\bar{L}) = \frac{1}{\frac{1}{\epsilon_1^2} + \frac{1}{\epsilon_2^2}}$$

*Corrected for difference in absorber between the chamber and final coincidence counter for the two cases.

**Corrected for the protons passing through 30 cm of lead without nuclear interaction.

L computed above, equation 5 can be solved for N_o to obtain the total number of protons incident on the absorber. The two highest momentum values for the 15 and 30 cm cases and the three highest momentum values for the 5 cm case were corrected in this manner in arriving at the total proton intensities in Figure VII.

D. Positive Excess for Mesons

With the foregoing determination of the proton component it is possible to compute the positive excess for mesons alone. Use is made of the work of Potter (3) which gives the spectra of all positive and negative particles at 3.4 km. The positive excess is assumed to be due to the presence of protons and to a positive excess of mesons. Therefore, subtraction of the protons from the positive particles leaves only positive mesons. Dividing the intensity of the positive mesons by that of the negative mesons gives the positive excess for mesons.

One value for the meson positive excess can be obtained in the interval 0.17 to 0.60 Bev/c from the 30 cm case. In this interval both mesons and protons were stopped by ionization losses. The observed heavy track intensity was subtracted from the intensity of positive particles to give, in the manner stated above, a meson positive excess of $1.14 \pm .07$. Another determination can be made in the momentum interval 0.60 to

2.0 Bev/c. Here the total proton intensity, which was obtained in Section B, was used to calculate a positive excess of 1.17 $\pm$ .06.

E. Comparison with Results of Other Investigators

1. Whittemore and Shutt (14). An experiment was performed at 3.4 kilometers altitude using two cloud chambers with a magnetic field between. In the lower chamber were placed lead absorbers to aid in the energy determination. A three-fold coincidence, using very thin walled tubes at atmospheric pressure, formed a telescope for selection of particles in a vertical direction. All particles with heavy tracks stopping in a 6 cm absorber in the lower chamber were considered to be protons. The proton intensities thus determined have been plotted, along with the present values, in Figure VIII. The work of Whittemore and Shutt involves a much lower momentum cut-off than the present investigation. Their intensities near 0.5 Bev/c are higher than any intensity found in the present investigation, but occur below the absorption cut-off of the present work. Near 0.7 Bev/c the intensities of Whittemore and Shutt agree well with the present values. At higher momenta their intensities are without meaning as protons cannot be recognized by track density at such high momenta.

Whittemore and Shutt have also calculated the proton intensity at higher momenta under the assumption that the positive excess of mesons remains constant as these mesons travel from 3.4 kilometers to sea level. Thus, they determined the proton intensity at 3.4 kilometers by using a meson positive excess obtained from that at sea level. Their estimates extend to much higher momenta (7 Bev/c) than the present investigation, but with much poorer statistics. Within statistics the results agree with the present investigation.

Mylroi and Wilson (18). By means of a counter-absorber arrangement placed below a magnetic spectrograph they measured the momenta at sea level of all particles stopping in 5, 10, 15 and 20 cm of lead. Protons and mesons were separated by the same method as used in the present work. They obtained a value for L of 160 ± 40 g/cm^2. However, close examination of their data as presented in the reference shows that the standard deviation for two of the three values computed was estimated incorrectly. Doing this correctly and taking an average of the three values gives a result of 136 ± 55 g/cm^2.

This rather low value can be easily explained. Of the three values computed, two are too inaccurate to have much effect on the average. The third is for the momentum interval 0.67 to 1.0 Bev/c. It is very likely that this interval con-

tains many protons whose momentum exceeds the 0.66 Bev/c needed to pass through the 5 cm of lead, but which undergo enough scattering so that they are stopped in the lead. Inclusion of these scattered particles results in a low value for L. Calculation of L for the same momentum interval from data in the present experiment would also give such a low result.

3. Froehlich, Harth and Sitte (19). Using a multiple plate cloud chamber with a counter-absorber hodoscope below to measure the range, a value for L of 190 $\pm$ 15 g/cm^2 was obtained for nuclear interacting particles with momentum less than 2.85 Bev/c. The events recorded as nuclear interactions were: (1) penetrating showers with ionizing primary and two or more secondaries, (2) stars with one or more heavy prongs, and (3) large showers containing heavy prongs.

4. Meson positive excess. Table V below gives a comparison of the values of meson positive excess obtained here and by others at nearly the same altitude.

TABLE V

MESON POSITIVE EXCESS

Investigator	Method	Momentum in Bev/c	Positive Excess
This Experiment	Cloud chamber	0.17-0.60	1.14 ± .07
		0.60-2.00	1.17 ± .06
Charbonnier (12)	Cloud chamber	0.34-1.0	1.09 .06
		1.0 -1.67	1.21 .08
		1.67-	1.22 .07
Whittemore and Shutt (14)	Cloud chamber	0.3 -0.7	1.35 .10
Brode (17)	Magnetic lens	1.0 -2.5	1.30 .03
Quorcia (16)	Magnetic lens	0.23-	1.13 .01
Bernardini (15)	Magnetic lens		1.20

Attempts to correlate the various values for the positive excess with method or momentum have been unsuccessful. The high values cannot be attributed to protons since Whittemore and Shutt obtained and subtracted from the positive particles a proton intensity comparable to that obtained in this experiment, and Brode measured particles passing through 60 cm of iron.

PART VIII

ERRORS AND CRITICISMS

1. Explanation of Blank Photographs. Not all photographs in the present investigation show single proton or meson tracks. Due to failure of the Al counters to provide adequate shower protection, some photographs show shower-type events which are recognized from the multiplicity of tracks and the occurrence of very low momentum particles of minimum ionization which are certainly electrons. Other photographs do not show any evidence of a track and are referred to as misses. As careful investigation has shown, these are not due to some failure of the equipment, but represent actual C-A events in which no charged particle traverses the chamber. Conclusive evidence also shows that they cannot be explained as occasional failure of the chamber to produce tracks. Rather, they must be attributed to showers which have actuated the C-tubes and failed either to actuate the A-tubes or to give a track in the chamber. As a counter will be triggered on production of a single ion pair while occurrence of a chamber track requires concentrated production of many such pairs, the two devices are not equivalent in their response. These misses are then thought to be due to low energy

gamma radiation (associated with showers but not accompanied by higher energy electrons) capable of actuating a Geiger counter but incapable of producing a cloud chamber track.

2. Inclusion of Electrons. From the standpoint of the present experiment it is important to show that there is small probability of obtaining a single electron track of energy greater than 100 Mev which could not then be distinguished from a meson. The small frequency of occurrence of single tracks of angle beyond the counter telescope acceptance limits and absence of tracks below the absorption cut-off in other experiments with this equipment (3,4,12) show the number of single electron tracks photographed to be small even compared to the statistical uncertainty of the meson intensities. It may seem odd that showers often show up as either multiple tracks or blank photographs but rarely as single tracks. However, appearance of at least one electron track of energy greater than 100 Mev almost assures, according to fairly well established shower theory, that it will be accompanied by other tracks, thus the data probably include very few electrons.

PART IX

SUMMARY

The proton momentum spectrum at elevation 3.4 kilometers and magenetic latitude 48 degrees north has been given in Figure VIII. It is considered to be valid for the momentum interval 0.7 to 2.0 Bev/c and agrees at the lower end of the interval with that obtained by Whittemore and Shutt (14). Comparison with the total intensity obtained by Potter (3) shows that protons form 20 $\pm$ 2% of all ionizing particles (except electrons) in this momentum interval. It should be noted that this is an average value for the interval from 0.7 to 2.0 Bev/c. At 2.0 Bev/c the proton component is only 10% of the total radiation.

The mean free path for removal of protons by nuclear interaction in lead has been computed as 206 $\pm$ 30 g/cm^2 for protons of momentum between 0.9 and 2.5 Bev/c, and the result compared with those of other investigators.

The determination of the meson positive excess has been included in an effort to report all available information provided by the data. The result, as shown in Table V, is in favor of the low values obtained by Charbonnier (12) and Quercia (16). The wide spread of the results obtained by all investigators is unexplained.

BIBLIOGRAPHY

1. D. E. Miller, J. E. Henderson, D. S. Potter, and Jay Todd, Jr. Phys. Rev. 79:459 (1950).

2. C. E. Miller, J. E. Henderson, D. S. Potter, and Jay Todd, Jr. Phys. Rev. 84:981 (1951).

3. D. S. Potter. Ph. D. thesis, University of Washington, 1951.

4. Jay Todd, Jr. Ph. D. thesis, University of Washington, 1952.

5. C. D. Anderson and S. H. Neddermeyer. Phys. Rev. 50: 263 (1936).

6. W. M. Powell. Phys. Rev. 69:385 (1946).

7. R. V. Anderson, et al. Rev. Med. Phys. 20:334 (1948).

8. F. C. Brown and J. C. Street. Phys. Rev. 84:1183 (1951).

9. B. Rossi. Rev. Med. Phys. 20:357 (1948).

10. K. Greisen. Phys. Rev. 61:212 (1949).

11. D. J. X. Montgomery. Princeton University Press, 1949.

12. F. M. Charbonnier. Ph. D. thesis, University of Washington, 1952.

13. M. Correll. Phys. Rev. 72:1055 (1947).

14. W. L. Whittemore and R. P. Shutt. Phys. Rev. 86:940 (1952).

15. G. Bernardini, M. Pancini, E. Conversi, E. Scrocco, and G. C. Wick. Phys. Rev. 68:109 (1945).

16. I. F. Quercia, et al. Nueve Cim. 7:277 (1950).

17. R. B. Brode. Phys. Rev. 76:468 (1949).

18. M. G. Mylroi and J. G. Wilson. Proc. of Phys. Society Sec. A64:417 (1951).

19. F. E. Froehlich, E. M. Harth, and K. Sitte. Phys. Rev. 87:504 (1952).

20. W. W. Brown and A. S. McKay. Phys. Rev. 77:342 (1950).